Characterization of a Streptococcal Cholesterol–Dependent Cytolysin with a Lewis y and b Specific Lectin Domain †

8 AUTHORS, INCLUDING:

Characterization of a Streptococcal Cholesterol-Dependent Cytolysin with a Lewis y and b Specific Lectin Domain[†]

Stephen Farrand[‡], **Eileen Hotze**[‡], **Paul Friese**[§], **Susan K. Hollingshead**[||], **David F. Smith**[⊥], **Richard D. Cummings**[⊥], **George L. Dale**[§], and **Rodney K. Tweten**[*,‡]

Department of Microbiology and Immunology and Department of Medicine, University of Oklahoma Health Sciences Center, Oklahoma City, Oklahoma 73104, Department of Microbiology, University of Alabama at Birmingham, Birmingham, Alabama 35294-2170, and Department of Biochemistry, Emory University School of Medicine, Atlanta, Georgia 30322

Abstract

The cholesterol-dependent cytolysins (CDCs) are a large family of pore-forming toxins that often exhibit distinct structural changes that modify their pore-forming activity. A soluble platelet aggregation factor from *Streptococcus mitis* (Sm-hPAF) was characterized and shown to be a functional CDC with an amino-terminal fucose-binding lectin domain. Sm-hPAF, or lectinolysin (LLY) as renamed herein, is most closely related to CDCs from *Streptococcus intermedius* (ILY) and *Streptococcus pneumoniae* (pneumolysin or PLY). The LLY gene was identified in strains of *S. mitis*, *S. pneumoniae*, and *Streptococcus pseudopneumoniae*. LLY induces pore-dependent changes in the light scattering properties of the platelets that mimic those induced by platelet aggregation but does not induce platelet aggregation. LLY monomers form the typical large homooligomeric membrane pore complex observed for the CDCs. The pore-forming activity of LLY on platelets is modulated by the amino-terminal lectin domain, a structure that is not present in other CDCs. Glycan microarray analysis showed the lectin domain is specific for difucosylated glycans within Lewis b (Le^b) and Lewis y (Le^y) antigens. The glycan-binding site is occluded in the soluble monomer of LLY but is apparently exposed after cell binding, since it significantly increases LLY pore-forming activity in a glycan-dependent manner. Hence, LLY represents a new class of CDC whose pore-forming mechanism is modulated by a glycan-binding domain.

The viridans streptococci, which include *Streptococcus mitis*, *Streptococcus mutans*, *Streptococcus salivarius*, and *Streptococcus sanguis*, are normally found as members of the normal flora of the oropharyx. These organisms can escape this niche, however, and cause a variety of diseases that include infective endocarditis, bacteremia, and septicemia. *S. mitis* is one of the more common isolates, and its antibiotic resistance is increasing, making treatment of its infections difficult (1–4). *S. mitis* was recently associated with a large outbreak of a toxic shock-like syndrome that affected thousands of individuals in China (5). *S. mitis* is typically not considered to be toxigenic, and it is characterized by an α-hemolytic phenotype. Jeffries et al. (6), however, recently showed that some *S. mitis* strains express a cholesterol-dependent cytolysin (CDC), designated mitilysin (MLY), which is nearly identical to *Streptococcus pneumoniae* pneumolysin. Another potential *S. mitis* pathogenesis factor is human platelet

[*]Corresponding author. Phone: (405) 271-1205ext 1. Fax: (405) 271-3117. E-mail: rod-tweten@ouhsc.edu.
[‡]Department of Microbiology and Immunology, University of Oklahoma Health Sciences Center.
[§]Department of Medicine, University of Oklahoma Health Sciences Center.
[||]Department of Microbiology, University of Alabama at Birmingham.
[⊥]Department of Biochemistry, Emory University School of Medicine.

aggregation factor (Sm-hPAF)[1] that was purified from *S. mitis* isolated from a patient with Kawasaki disease (7). This protein was shown to aggregate human platelets and was designated *S. mitis* human platelet aggregation factor or Sm-hPAF. More recently, Ohkuni et al. (8) showed that antibody titers to a Sm-hPAF-derived peptide were significantly elevated in children with Kawasaki disease, a disease that is often associated with platelet aggregation and coronary artery thrombosis.

The peptide sequence reported by Ohkuni et al. (8) was derived from the sequence for a Sm-hPAF gene from *S. mitis* Nm-65 recently reported in GenBank (accession number AB051299.1). The sequence of Sm-hPAF encodes a predicted CDC structure that is most closely related to inter-medilysin (ILY), the CDC from *Streptococcus intermedius* (9). The DNA-derived primary structure of Sm-hPAF exhibits an extra amino-terminal domain of about 162 amino acids. Based on the DNA-derived primary structure, this domain is related to the European eel *Anguilla anguilla* agglutinin (AAA), a fucose-binding lectin that preferentially binds glycans containing fucosylated structures found in the blood group antigens A, B, H, and Lewis a (Le[a]) (10,11).

Herein we describe the properties of purified recombinant Sm-hPAF (*referred to as lectinolysin or LLY hereafter*) from *S. mitis* SK597. These studies show that LLY is a pore-forming CDC with a functional glycan-binding domain. LLY does not trigger platelet aggregation but does form pores in platelet membranes. The isolated fucose-binding lectin domain of LLY exhibits specificity for glycans containing the Lewis y (Le[y]) and b (Le[b]) antigens. The lectin domain of LLY appears to modulate the pore-forming activity of LLY in a glycan-dependent manner after LLY binds to the cell surface.

METHODS

Bacterial Strains, Plasmids, and Chemicals

The full-length gene for LLY was cloned by PCR from the chromosomal DNA of *S. mitis* strain SK597 using the primer ATGAATCAA-GAAAAACGTTTGCATCGCTTTGTCAAAAAG, and the reverse primer sequence was 5′-TTACTCATTCACAATTTTTTCAT-CAACTTTAGGGTTTAG. For purposes of expression the cloned LLY gene was amplified with the primers 5′-TC**G-GATCC***GAG*CAAGGGAATCGTCCAGTTG that introduced a 5′ *Bam*HI endonuclease site and 5′-CT**GAATTC***TTA*CT-CATTCACAATTTTTTCATCAACTTTAGGG that placed a 3′ *Eco*RI endonuclease after the stop codon at the 3′ end of the gene. These primers removed the signal peptide and placed the gene for the secreted LLY in-frame in the pTrcHisA vector (Invitrogen). ILY and PFO were previously cloned into pTrcHisA as described (12,13). All mutations were made in the native LLY (naturally cysteine-less), ILY (naturally cysteine-less), or cysteine-less PFO (PFO[C459A]) background. All chemicals and enzymes were obtained from Sigma, VWR, or Research Organics. All fluorescent probes were obtained from Molecular Probes (Invitrogen).

Generation and Purification of Recombinant LLY, ILY, and PFO and Their Derivatives

Using PCR QuikChange mutagenesis (Stratagene), various amino acid substitutions were introduced into native LLY, ILY, or PFO[C459A]. The Oklahoma Medical Research Foundation Core DNA Sequencing Facility performed all DNA sequence analysis. The expression and purification of recombinant LLY, ILY, PFO, and their derivatives from *Escherichia coli* were performed as described (13,14). Purified protein was dialyzed into buffer [300 mM NaCl, 10 mM MES, 1 mM EDTA (pH 6.5)] overnight at 4 °C, made 5 mM in dithiothreitol (DTT) and

---

[1]Abbreviations: ILY, intermedilysin; PLY, pneumolysin; PFO, perfringolysin; Sm-hPAF, *Streptococcus mitis* human platelet aggregation factor; EC$_{50}$, half-maximal effective concentration.

10% (v/v) sterile glycerol, and stored at −80 °C. For mutants that contained an engineered disulfide bridge the DTT was left out of the storage buffer.

PCR Screening Streptococci for the LLY Gene

Primers were used in the PCR amplification at a 20 pmol final concentration. These primers were designed to amplify out the entire coding sequence for the LLY gene. The forward primer sequence was 5′-ATGAATCAAGAAAAACGTTTG-CATCGCTTTGTCAAAAAG, and the reverse primer sequence was 5′-TTACTCATTCACAATTTTTTCATCAACTT-TAGGGTTTAG. Chromosomal DNA from each streptococcal strain was prepared using the Invitrogen Easy DNA kit, and 100 ng was added to the PCR reaction. An additional 2 μL of 25 mM $MgCl_2$ was added to Qiagen Master Mix for a final PCR volume of 25 μL. Each PCR product was separated on a 1% agarose gel.

Chemical Modification of LLY and Its Derivatives with Sulfhydryl-Specific Fluorescent Probes

The cysteine derivatives of LLY and LLY[Lec] were modified with Alexa Fluor 488 C_5-maleimide (Invitrogen) via the sulfhydryl group as previously described (12). Modified protein stocks were adjusted to 10% (v/v) sterile glycerol, quick frozen in liquid nitrogen, and stored at −80 °C. Proteins were labeled at an efficiency of 75% or greater.

K_d Determination

Fluorescein-labeled glycans were prepared as previously described using free reducing oligosaccharides (15). The K_d of the interaction of LLYLec with Ley was determined by fluorescence anisotropy. Fluorescence measurements were carried out using an SLM 8100 fluorometer equipped with excitation and emission calcite polarizers. The excitation and emission monochromator wavelengths were set to 480 and 520 nm, respectively. The excitation and emission bandpass was set to 4 nm. Sample volume was maintained at 300 μL in a Starna microcell with a total capacity of 560 μL. Temperature was maintained at 23 °C. The fluorescein-labeled Le[y] was maintained at 167 nM, and the LLY[Lec] was varied from 300 nM to 120 μM. The anisotropy (r) was calculated at each concentration of LLY from the equation:

$$r = \frac{I_{VV} - GI_{VH}}{I_{VV} + 2GI_{VH}}$$

I is intensity, V is vertically polarized light, and H is horizontally polarized light. The G factor ($G = I_{HV}/I_{HH}$) was calculated for each sample. The Δr was plotted versus the concentration of LLY, and the dissociation constant (K_d) was calculated using the equation $Y = B_{max}X/(K_d + X)$ for one site binding, where B_{max} is the maximal binding and the K_d is the concentration of ligand (in this case the LLY) necessary to achieve half-maximal binding. Data analysis was carried out using Graphpad Prism software.

Platelet Aggregation Assay

Platelet-rich plasma (PRP) was prepared from normal human donors as described previously (16). Blood donors were free of aspirin or other antiplatelet medications for at lease 7 days prior to donation. Aggregation experiments were performed with a Model PAP-4 aggregometer from Bio/Data Corp. Total reaction volume was 200 μL. Convulxin-induced aggregation (500 ng/mL final concentration (16)) was used as a positive control. LLY was assayed at 71 nM, LLY[CDC] at 95 nM, and LLY[Lec] at 280 nM.

Calcein Release Assay

PRP was diluted 1:100 with HEPES/saline assay buffer (2 mM $CaCl_2$, 1 mM $MgCl_2$, 150 mM NaCl, 10 mM HEPES, pH 7.5) and incubated with 2 μM calcein acetoxy methyl ester

(Molecular Probes, Eugene, OR) for 10 min at room temperature as previously described (17). LLY (0.7–2.9 nM) was incubated with the calcein-loaded PRP for 10 min at room temperature. Samples were then diluted with HEPES/saline and analyzed on a FACS-Calibur flow cytometer (Becton-Dickinson) using settings as described previously (17). Cells losing calcein fluorescence were quantified as a percentage of total platelets.

The EC_{50} values for LLY- and LLYCDC-dependent calcein release were calculated using a nonlinear sigmoidal dose–response curve fit of the data (Prism Software).

Glycan Microarray Binding Assay and Scanning

Glycan microarrays were prepared as described previously (33,37) and obtained from the NIH/NIGMS-funded Consortium for Functional Glycomics (see http://www.functionalglycomics.org/static/index.shtml). Before assay, the slides were re-hydrated for 5 min in TSM buffer (20 mM Tris-HCl, 150 mM sodium chloride (NaCl), 0.2 mM calcium chloride ($CaCl_2$), and 0.2 mM magnesium chloride ($MgCl_2$)). Alexa-488-labeled LLY^{Q190C} and its derivatives were used in the binding assay (560–640 nM), and the bound proteins were detected directly via the fluorescent tag.

The slides were scanned with a Perkin-Elmer ProScanarray MicroArray scanner (Waltham, MA) using an excitation wavelength of 488 nm. ImaGene software (BioDiscovery, Inc., El Segundo, CA) was used to quantify fluorescence. The data are reported as average relative fluorescence units (RFU) from four of the six replicates (after removal of the highest and lowest values) for each glycan represented on the array. Versions 2.1 and 3.0 of the printed array were used in these studies, and a complete list of glycans printed on these arrays can be found at the Functional Glycomics Gateway Web site: www.functionalglycomics.org/static/consortium/resources/resourcecoreh10.shtml.

SDS–Agarose Gel Electrophoresis (SDS–AGE)

SDS–AGE of monomer and oligomer species of the various CDCs was carried out as previously described (18).

Liposome Preparation

Cholesterol–phosphatidylcholine (55/45 mol %) liposomes were prepared as previously described (13). Lipids and cholesterol were obtained from Avanti Polar Lipids.

RESULTS

The Primary Structure of LLY

The LLY gene was cloned from *S. mitis* SK597, which exhibits characteristics of both *S. mitis* and *Streptococcus oralis* (Hollingshead, unpublished data). The gene sequence (see GenBank accession number EU597013) exhibits the typical AT-rich (60% A–T) sequence of streptococcal genes. The deduced primary structure of LLY is nearly identical to the GenBank sequence for Sm-hPAF from *S. mitis* Nm-65 (accession number AB051299.1); 12 mostly conservative amino acid differences were identified (Figure 1a). These differences did not result from PCR-generated errors in the LLY sequence reported herein; the same sequence was derived from the cloned products of two separate PCR amplification experiments. Hence, the primary structure of LLY can apparently vary to some extent. The open reading frame encodes a protein with a mass of 73780.3 Da. Based on the previously published amino-terminal sequence of purified protein from the supernatant of *S. mitis* NM-65 (7) the amino terminus of secreted LLY is located at or near Thr-37, which is preceded by a 36-residue peptide that exhibits a typical type II signal peptide structure. The primary structure of LLY from residue 199 to 665 (Figure 1a) is most closely related to CDCs from *S. intermedius* (ILY) and *S.*

pneumoniae (PLY). The CDC structure of LLY also contains an undecapeptide sequence (EKTGLVWEP-WR) that is similar to the hallmark consensus sequence (ECTGLAWEWWR) found in most CDCs but contains substitutions at positions similar to those found in ILY (GATGLAWEPWR).

Unlike other characterized CDCs LLY contains an extra 162-residue peptide fused to its amino terminus (excluding the signal peptide) (Figure 1a). This peptide region exhibits similarity with the *A. anguilla* (European eel) agglutinin (AAA) (33% identity) (10) (Figure 1b) and the carboxy-terminal carbohydrate-binding module of a putative member of the family 98 glycoside hydrolases from *S. pneumoniae* (47% identity) (Figure 1c) (19). Both proteins are fucose-binding proteins that exhibit a preference for glycans containing the H-antigen structure (Fucα1–2Galβ1–3(4)-GlcNAc-R).

Distribution of the LLY Gene

A collection of 165 strains of mostly *mitis* group streptococci was examined for the presence of the LLY gene by PCR using primers that encompassed its complete coding region. From this collection, twelve *S. mitis* strains, one *S. pneumoniae*, four *Streptococcus pseudopneumoniae*, and three *S. mitis/oralis* strains carried the gene. The PCR product size did not vary in size for any of the positive strains and comigrated with the 2 kb marker, consistent with its 1998 base pair sequence (including the stop codon) (data not shown). We confirmed expression and secretion of LLY in the SK597 strain (data not shown) that served as the source of the gene for our studies but have not confirmed its expression in the other species and strains that appear to carry the gene.

Hemolytic Activity of LLY and Derivatives

The coding region for LLY was cloned, expressed in *E. coli*, and purified (see Methods). Shown in Table 1 is the HD_{50} (dose of toxin required for 50% hemolysis under standard conditions; see Methods) for purified LLY, LLY^{CDC} (LLY lacking the amino-terminal lectin domain), PFO, and ILY. In Table 1 are the HD_{50} values, using human erythrocytes, for LLY and LLY^{CDC} and, for comparison, those of PFO and ILY. All of the CDCs exhibit picomolar HD_{50} values, but it appears LLY and LLY^{CDC} are 4–5-fold less active than PFO and ILY. These values are within the typical range for these toxins and can vary depending on the cell type and species of origin. As described below, however, the amino-terminal lectin domain appears to exert a glycan-dependent enhancement of LLY activity with platelets.

Similar to other CDCs LLY and LLY^{CDC} also formed large oligomeric complexes on cholesterol-rich liposomes (Figure 2). LLY^{CDC} monomer (52147 Da) and oligomer migrated similarly to PFO monomer (52672 Da) and oligomer. The similarity in the mass of both proteins suggests that both form oligomers with similar numbers of monomers. In contrast to PFO and LLY^{CDC} the migration of the LLY oligomer was significantly retarded. The slower migration of LLY was likely due to the additional mass contributed by the amino-terminal lectin domain (17751 Da). The CDCs typically form oligomers of 35–40 monomers (20); thus the oligomer mass of LLY would be at least 600 kDa greater than that of LLY^{CDC} or PFO, consistent with its slower migration on the gel.

LLY and Other CDCs Do Not Aggregate Platelets

Ohkuni et al. (7) reported that LLY (Sm-hPAF) stimulated platelet aggregation in human platelet-rich plasma (PRP). Qualitative analysis of platelet aggregation is commonly determined using an aggregometer, an instrument that measures the decrease in the light scattering properties of PRP as platelets aggregate into large complexes. Aggregometer analysis herein also showed apparent LLY-dependent platelet aggregation resulting in the decreased light scatter by the platelets (Figure 3a). Similar results were observed with purified

LLY^{CDC}, demonstrating that the predicted amino-terminal fucose-binding lectin domain was not required for this activity (Figure 3a). Purified lectin domain (LLY^{Lec}) did not induce any change in the light scattering properties of the platelets (Figure 3a). To confirm the aggregometer measurements reflected platelet aggregation by LLY and LLY^{CDC}, we performed a microscopic examination of the platelets after treatment. Surprisingly, we could not identify any aggregated platelets (Figure 3b). By comparison, we observed large platelet aggregates in PRP treated with convulxin, a nonenzymatic glycoprotein from venom of *Crotalus durissus terrificus* that induces platelet aggregation. Although the aggregometer readings indicated that LLY and LLY^{CDC} could aggregate platelets, the microscopic examination did not support this interpretation. Although unlikely, it was possible that we simply missed the aggregates formed by LLY. Therefore, we quantified the relative levels of platelets in each preparation.

To measure the relative levels of platelets present in these mixtures, we utilized a flow cytometry based approach. PRP was either left untreated or treated in the aggregometer with 140 nM LLY or 500 ng/mL convulxin for 3 min at 37 °C with stirring. Aliquots of treated PRP were then incubated with FITC-labeled antiglycoprotein IIb/IIIa antibody, and platelet concentration was determined by flow cytometry. The relative platelet concentration in each sample was determined by the time required to accumulate 5000 events on the cytometer. If platelets aggregated into larger complexes, it would take longer to accumulate 5000 counts. If no significant aggregation occurs, then the time required for 5000 counts should be similar to untreated platelets. The LLY-treated and control (untreated) samples had nearly identical platelet concentrations (5000 counts/34 s and 5000 counts/31 s, respectively). In contrast, the convulxin-treated sample was significantly depleted of individual platelets (5000 counts/84 s). Hence, both convulxin and LLY induce changes in the light scattering properties of the platelets, but it is clear that LLY does not induce platelet aggregation. How then did LLY affect the light scattering properties of the platelets without aggregation?

The light scattering properties of cells often result from shape change and/or loss of cytoplasmic contents. For example, erythrocytes lose their light scattering properties upon pore formation by the CDC PFO (21). Pore formation in platelets was determined by monitoring calcein release from LLY-treated platelets. As shown in Figure 4, calcein is efficiently released in a dose-dependent manner from the platelets treated with LLY or with LLY^{CDC}, suggesting that each formed a membrane pore. The relative EC$_{50}$ for calcein release by both proteins was quantified below in the studies described in Figure 7, where we show that LLY exhibits variable activity on platelets from different donors.

To assess whether the observed change in light scattering properties of LLY in the aggregometer was dependent on pore formation, a mutant of LLY was trapped in the prepore complex by the introduction of an engineered disulfide, but which could be converted to the pore-forming oligomer by reduction of this bond. We previously showed a disulfide bridge between domains 2 and 3 of the CDC structure prevents membrane insertion of the transmembrane β-hairpins but not binding and assembly of the prepore oligomer (22). When the disulfide bridge was reduced, the transmembrane β-hairpins inserted into the membrane and formed the pore.

A prepore-locked mutant of LLY was generated by introducing cysteines for Gly-222 and Asn-351 (LLY$^{G222C/N351C}$), residues analogous to Gly-83 and Ser-217 of ILY and to Gly-57 and Ser-190 of PFO, which were shown previously to form a disulfide and trap both toxins in prepore complexes (ref 22 and Soltani and Tweten, unpublished data). LLY$^{G222C/N351C}$ functioned as expected; when the disulfide bond was oxidized, it was not hemolytic, whereas reduction of the disulfide restored near native hemolytic activity (data not shown). Treatment of PRP with oxidized LLY$^{G222C/N351C}$ did not elicit a change in the light scattering properties

of the platelets (Figure 5a), but reduction of the disulfide bond restored this activity. Similarly, the oxidized disulfide-locked variants of ILY (Figure 5b) and PFO (Figure 5c) did not change the light scattering properties of the platelets, whereas the reduced forms of each triggered significant changes. These data show that the changes in light scattering properties of platelets are dependent on the pore-forming properties of LLY, PFO, and ILY and are not the result of platelet aggregation.

Glycan Specificity and Affinity of the LLY Lectin Domain

We next determined if the putative fucose-binding lectin domain of LLY was functional. A glycan microarray of vertebrate-type glycans (see Methods for a link to the complete list of glycans on this array) was probed with fluorescently tagged LLY. The probe consisted of the cysteine-substituted mutant LLY[Q190C] labeled with the maleimide derivative of Alexa-488 via the cysteine sulfhydryl (LLY[Q190C-Alexa]). Gln-190 was chosen for substitution with cysteine since it is located at the junction of the CDC and lectin domains. When the glycan microarray was probed with LLY[Q190C-Alexa], no significant binding was detected (Figure 6a). This result suggested several possibilities: the lectin domain might bind to glycans that were not represented in the array, the lectin domain was not functional, or the glycan-binding site was sterically occluded or somehow inhibited in the soluble monomer of LLY.

We first tested the latter possibility, primarily because of the amino-terminal location of the lectin domain. This location positions the lectin domain distal to the carboxy-terminal domain 4, which contains the membrane-binding site of the CDCs (23–26). If the glycan-binding site was exposed in the monomer, it could bind LLY to cells in an unfavorable orientation, preventing critical domain 4 membrane interactions that initiate a cascade of ordered structural changes in the CDCs that lead to pore formation (reviewed in ref 27). Therefore, in this scenario occlusion or inhibition of the glycan-binding site may be necessary until after LLY has bound to the membrane. If correct, then expression of the lectin domain alone should restore its binding activity. A pair of stop codons was introduced after residue 190 of LLY[Q190C] to eliminate the translation of the downstream CDC structure. This construct was designated LLY[Lec-Q190C].

Purified LLY[Lec-Q190C] was fluorescently labeled with Alexa-488 and used to probe the glycan microarray. As shown in Figure 6b, we observed significant binding to several glycans on the microarray. We also determined whether binding to the glycans on the glycan microarray was lost if we changed a residue that has been shown to be conserved in the fucose-binding site of related lectins. The AAA glycan binding site contains three key residues that make polar contacts with the fucose molecule. The Nε of His-52 contacts O-5 of the fucose ring whereas the guanidinium groups of Arg-79 and Arg-86 make contact with 3-OH and 4-OH ring hydroxyls of fucose (10). These residues are also conserved in the fucose-binding site of the family 98 glycoside hydrolases from *S. pneumoniae* (SP2159) (19) and correspond to residues His-85, Arg-112, and Arg-120 of LLY, respectively (Figure 1b,c). Arg-112 of LLY[Lec] was changed to Ala in LLY[Lec-Q190C]. This mutant (LLY[Lec-Q190C/R112A]) was labeled with Alexa-488 at Cys190 and used to probe the glycan microarray. This mutation eliminated the glycan binding activity of LLY[Lec] (Figure 6c), consistent with the conservation of this active site residue.

We further investigated the binding of LLY[Lec] to the glycan microarray to determine its glycan specificity. We probe the microarray with three different concentrations of LLY[Lec] that spanned a 100-fold range of concentration from 5.6 to 560 nM. These results (Table 2) are shown for all glycans bound at the highest concentration of LLY[Lec] and selected glycans representative of those not bound by LLY[Lec] at the highest concentration of LLY[Lec] (representative of most glycans on the array). When the array was probed at 560 nM LLY[Lec], it bound to glycans containing the H-antigen structure (Fucα1–2Galβ1–3(4)GlcNAc-

R) as found within the A, B, O, Le^y, and Le^b blood group antigens (Table 2, glycan IDs 1–24) and showed little affinity for the nonfucosylated type 1 and type 2 oligosaccharides (Table 2, glycan IDs 33–38), fucosylated glycans that did not contain the H-antigen, including Le^a and Le^x containing structures (Table 2, glycan IDs 27–32), and the difucosylated structures (Table 2, glycan IDs 42–50). At this high concentration of LLY^{Lec}, we observed some weak binding to irrelevant glycans (Table 1, glycan IDs 39–41). However, when the microarray was probed with 10-fold (56 mM) and 100-fold lower (5.6 nM) concentrations of LLY^{Lec}, we observed a marked shift in binding preference for glycans containing Le^y and Le^b antigens (Table 2, glycan IDs 1–7). These results demonstrate that LLY^{Lec} has a unique recognition of difucosylated glycans Fucα1–2Galβ1–3/4(Fucα1–4/3)GlcNAc-R) as found in Le^b and Le^y blood group antigens. Interestingly, glycans 6 and 7 are such difucosylated glycans, which also contain the blood group B and A determinants, respectively. However, as noted above, when the array is probed at the lowest concentration of LLY^{Lec}, it binds weakly or not at all to blood group B (Galα1–3[Fucα1–2]Galβ1–3/4R), blood group A (GaNAclα1–3[Fucα1–2]Galβ1–3/4R), or blood group H (Fucα1–2Galβ) determinants that lack the necessary difucosylated structures.

The affinity of LLY^{Lec} for Le^y was determined by measuring changes in fluorescence anisotropy (Δr) of fluorescently tagged Le^y as the concentration of LLY^{Lec} was varied. From this analysis the K_d of the LLY^{Lec}-Le^y interaction was determined to be approximately 38 μM (Figure 6d). As expected from the microarray data, Le^x antigen, which lacks the H-antigen structure, was not bound significantly (<10% of Le^y) at the highest concentration of LLY^{Lec}.

The Lectin Domain of LLY Modulates Its Pore-Forming Activity

Ohkuni et al. (7) previously showed that platelets of some donors were unresponsive to Sm-hPAF-mediated aggregation (shown herein to be due to pore-dependent changes in platelet light scattering properties). This observation suggested that different donor platelets might exhibit different susceptibilities to the pore-forming activity of LLY. Consistent with this prediction, we observed that platelets from different donors exhibited differential susceptibility to LLY (Dale and Friese, unpublished observations). Shown in Figure 7a is the EC$_{50}$ for LLY pore formation determined on high (donor 1) and low (donor 3) sensitivity platelets. The platelets from donor 1 are nearly 6-fold more sensitive to LLY (EC$_{50}$ = 4.890×10^{-11}) than those from donor 3 (EC$_{50}$ = 2.88×10^{-10}). These results suggested that a feature of donor 1 platelets significantly enhanced their susceptibility to LLY.

We hypothesized that enhancement of LLY activity resulted from a glycan-dependent interaction of the lectin domain after monomer bound the cell surface. If correct, then preincubating platelets with LLY^{Lec} should prevent interaction of the lectin domain of LLY with surface glycans and block the enhancement of LLY activity on the highly sensitive donor 1 platelets. The EC$_{50}$ for calcein release by LLY from platelets pretreated with LLY^{Lec} (EC$_{50}$ = 3.8×10^{-10}) was approximately 8-fold higher than the EC$_{50}$ for LLY on platelets that were not pretreated with LLY^{Lec} (EC$_{50}$= 4.890×10^{-11}) (Figure 7a). Similar results were observed if the platelets were incubated with 50 mM fucose instead of LLY^{Lec} but not with 50 mM sucrose as a control (data not shown). Furthermore, pretreatment of the low sensitivity donor 3 platelets with LLY^{Lec} had little impact on the activity of LLY, suggesting that the glycan(s) was largely absent from this donor's platelets. The results show the lectin domain increases LLY specific activity, apparently by interacting with one or more glycans on the cell surface of platelets.

These data also predict LLY^{CDC}, which lacks the lectin domain, should be less active than LLY on donor 1's platelets. To test this prediction, the EC$_{50}$ for calcein release by LLY and LLY^{CDC} was determined. As is shown in Figure 7b the EC$_{50}$ for LLYCDC on donor 1 platelets was 7-fold higher than the EC$_{50}$ for LLY, consistent with the change observed in LLY activity

on LLY^{Lec}-pretreated donor 1 platelets. Furthermore, LLY^{CDC} platelet pore-forming activity was not affected by preincubating the platelets with LLY^{Lec} (Figure 7c).

DISCUSSION

The studies herein show LLY is a functional CDC with an amino-terminal fucose-binding lectin domain. The LLY gene was detected in various isolates of the *mitis* group of the streptococci. This was not surprising, since there is evidence for the extensive exchange of genetic material between these species (28) and recently it has been shown that some *S. mitis* strains carry a gene encoding a CDC nearly identical to pneumolysin (6). Hence, it is perhaps not unexpected that the LLY gene appears to be present in one isolate of *S. pneumoniae*. LLY exhibits the typical large oligomeric membrane complexes and pore-forming activity of the CDCs. Pore formation in the platelet membrane was shown herein to be responsible for changes in their light scattering properties rather than the previously reported aggregation (7). The primary structure of LLY is distinct from other CDCs due to the presence of an amino-terminal fucose-binding lectin domain. The isolated lectin domain binds to glycans that contain H-antigen structure (Fucα1–2Galβ1–3(4)GlcNAc-R), with a marked preference for the difucosylated Le^y and Le^b antigens. The glycan binding site is occluded in the soluble LLY monomer but is apparently exposed after the monomer binds to the cell surface since it enhances LLY-dependent pore-forming activity through a glycan-dependent mechanism. To date, LLY is the only characterized CDC to exhibit a glycan-binding lectin domain.

The glycan-binding site is occluded in the soluble LLY monomer, presumably to prevent nonproductive interactions that would inhibit the assembly of the oligomeric pore complex. Previous studies showed that the CDC monomer is bound in a perpendicular orientation to the membrane surface via loops at the tip of domain 4, an interaction that initiates ordered conformational changes in the CDC structure necessary for pore formation (reviewed in ref 27). The amino-terminal location of the lectin domain places it next to domain 1 of the CDC structure and distal to the membrane-binding site in domain 4 (Figure 8). If the glycan-binding site was exposed in the soluble monomer, its interaction with a surface glycan could bind LLY to the surface in a nonproductive orientation that would prevent the assembly of the oligomeric pore complex. Yet, as described below, the glycan-binding site must be exposed after LLY binds to the membrane surface, since it enhances pore-forming activity.

Although caution must be used in extrapolating conclusions from molecular models, they suggest a possible explanation for the occlusion of the glycan-binding site in LLY. The structural model of the LLY^{Lec}, based on the crystal structure of the Le^y-binding module of *S. pneumoniae* family 98 glycoside hydrolase (19), positions the C-terminus of LLY^{Lec} on the same face as Arg-112, a residue we showed herein is conserved and essential for glycan binding. In LLY the carboxy-terminal lectin domain would be fused to the amino terminus of the CDC, orienting the binding site toward the upper surface of domain 1 of the CDC structure, potentially occluding the glycan-binding site. An assessment of the packing quality of the LLY^{CDC} structural model using ANOLEA (29) shows that residues in domain 1 (Figure 8), near the predicted site of interaction between the amino-terminal fucolectin domain and domain 1 of the CDC, exhibit a nonfavorable energy environment. This suggests that these residues do not pack similarly to the analogous residues in ILY. Hence, the residues in this region may adopt a different conformation in LLY so that they can specifically interact with the glycan-binding surface of the lectin domain in the soluble monomer.

Our studies revealed that platelets from different donors responded differently to LLY-dependent pore formation. Ohkuni et al. also observed a similar phenomenon in their aggregation experiments (7) (which we now know to be due to platelet lysis). The EC$_{50}$ for LLY on the platelets of a high responder donor was about six times lower than that observed

when the platelets from a low responder when they were treated with LLY. This difference was abolished if both sets of platelets were treated with the lectin-deficient LLY[CDC] or if high responder platelets were first treated with LLY[Lec] or L-fucose before adding ILY. When the high responder platelets were pretreated with LLY[Lec] to block its binding sites before the addition of LLY, we observed an approximately 8-fold increase in the EC_{50}. Hence, LLY exhibits an intrinsic pore-forming activity that is enhanced by the presence of the lectin domain, apparently in a glycan-dependent manner. The most likely explanation for the differences in platelet sensitivity is that the levels of glycan recognized by the lectin domain differ in platelets from various donors. Based on the array analysis Le[y] and/or Le[b] antigens are likely candidates for these differences, but we cannot rule out the possibility that other fucose-containing glycans mediate this interaction. The mechanistic stage of the LLY pore-forming mechanism that is modulated by the lectin domain is not yet known but apparently occurs after the initial domain 4-mediated cell binding. Most toxins that have a lectin-like domain use it to bind to glycan-containing receptors (30–36), whereas the LLY lectin domain does not appear to participate in receptor recognition.

The glycan microarray analysis showed Le[y] and Le[b] are preferred ligands of the LLY lectin, with the H-antigen itself being a weaker ligand. The H-antigen is expressed in many cells and tissues of all individuals, but expression of Le[y] and Le[b] antigens is more restricted in adults. Besides being on erythrocytes and in body secretions (e.g., saliva), they are expressed throughout the gastrointestinal tract but at levels that can differ based on location (37,38). Expression of both antigens may be highly upregulated on epithelial tumors of the GI tract (39,40). In normal tissue, Le[b] is highly expressed on mucosal surfaces of the fetal colon, but in adults its expression is restricted to the proximal colon (41). Le[y] is expressed strongly in proximal regions of the terminal ileum and cecum and weakly in the ascending colon and beyond (42). In addition, both Le[y] and Le[b] can be found weakly expressed in gastric mucosa (43). Le[y] is also expressed by some *Helicobacter pylori* isolates (44).

Interestingly, Le[y] is expressed at low levels in circulating human peripheral blood granulocytes but is upregulated upon their activation (45). Le[y]-expressing neutrophils are also found in the synovial fluid of patients with arthritic joint disease (46). The *mitis* group of streptococci is part of the normal flora of the oropharynx and nasopharyx, but as indicated in the introduction they are increasingly associated with antibiotic-resistant bacteremia or septicemia. The lectin-dependent enhancement of LLY activity may increase its activity toward Le[y]-expressing activated neutrophils, thus potentially blunting one of the early responses to infection.

In summary, these studies show that LLY is a member of the CDC family of pore-forming toxins and is the only identified CDC that has a glycan-binding lectin domain. The lectin domain exhibits a strong preference for Le[b] and Le[y] and modulates LLY pore-forming activity in a glycan-dependent manner after LLY has bound to the membrane. The mechanistic basis for this effect remains unknown. Finally, several species of streptococci appear to carry the gene for LLY. One *S. pneumoniae* isolate appeared to carry the gene for LLY, suggesting that there may be a subpopulation of this important pathogen that expresses LLY in association with PLY or it has been substituted for PLY.

Acknowledgements

References

1. Kennedy MJ, Jackson MA, Kearns GL. Delayed diagnosis of penicillin-resistant *Streptococcus mitis* endocarditis following single-dose amoxicillin prophylaxis in a child. Clin Pediatr (Philadelphia) 2004;43:773–776.

2. Gowda RM, Ansari AW, Khan IA. Complete endocardial cushion defect (complete atrioventricular canal) manifested in adult life by *Streptococcus mitis* endocarditis of the common atrioventricular valve. Int J Cardiol 2003;89:109–110. [PubMed: 12727016]

3. Hall GE, Baddour LM. Apparent failure of endocarditis prophylaxis caused by penicillin-resistant *Streptococcus mitis*. Am J Med Sci 2002;324:51–53. [PubMed: 12120826]

4. Huang IF, Chiou CC, Liu YC, Hsieh KS. Endocarditis caused by penicillin-resistant *Streptococcus mitis* in a 12-year-old boy, J. *Microbiol*. Immunol, Infect (China) 2002;35:129–132.

5. Lu HZ, Weng XH, Zhu B, Li H, Yin YK, Zhang YX, Haas DW, Tang YW. Major outbreak of toxic shock-like syndrome caused by *Streptococcus mitis*. J Clin Microbiol 2003;41:3051–3055. [PubMed: 12843042]

6. Jefferies J, Nieminen L, Kirkham LA, Johnston C, Smith A, Mitchell TJ. Identification of a secreted cholesterol-dependent cytolysin (mitilysin) from *Streptococcus mitis*. J Bacteriol 2007;189:627–632. [PubMed: 17071760]

7. Ohkuni H, Todome Y, Okibayashi F, Watanabe Y, Ohtani N, Ishikawa T, Asano G, Kotani S. Purification and partial characterization of a novel human platelet aggregation factor in the extracellular products of *Streptococcus mitis*, strain Nm-65. FEMS Immunol Med Microbiol 1997;17:121–129. [PubMed: 9061358]

8. Ohkuni, H.; Todome, Y.; Takahashi, H.; Nagamune, H.; Abe, J.; Ohtsuka, H.; Hatakeyama, H. Antibody titers to *Streptococus mitis*-derived human platelet aggregation factor (Sm-hPAF) in the sera of patients with Kawasaki disease. In: Sriprakash, KS., editor. Proceedings of the XVIth Lancefield International Symposium on Streptococci and Streptococcal Diseases. Elsevier B.V.; Palm Cove, Australia: 2006. p. 71-74.

9. Nagamune H, Whiley RA, Goto T, Inai Y, Maeda T, Hardie JM, Kourai H. Distribution of the intermedilysin gene among the anginosus group streptococci and correlation between intermedilysin production and deep-seated infection with *Streptococcus intermedius*. J Clin Microbiol 2000;38:220–226. [PubMed: 10618091]

10. Bianchet MA, Odom EW, Vasta GR, Amzel LM. A novel fucose recognition fold involved in innate immunity. Nat Struct Biol 2002;9:628–634. [PubMed: 12091873]

11. Majumder S, Roy A, Mandal C. Prediction of 3-D structures of fucose-binding proteins and structural analysis of their interaction with ligands. Glycoconjugate J 2004;20:545–550.

12. Giddings KS, Johnson AE, Tweten RK. Redefining cholesterol's role in the mechanism of the cholesterol-dependent cytolysins. Proc Natl Acad Sci USA 2003;100:11315–11320. [PubMed: 14500900]

13. Shepard LA, Heuck AP, Hamman BD, Rossjohn J, Parker MW, Ryan KR, Johnson AE, Tweten RK. Identification of a membrane-spanning domain of the thiol-activated pore-forming toxin *Clostridium perfringens* perfringolysin O: an α-helical to *β*-sheet transition identified by fluorescence spectroscopy. Biochemistry 1998;37:14563–14574. [PubMed: 9772185]

14. Soltani CE, Hotze EM, Johnson AE, Tweten RK. Specific protein-membrane contacts are required for prepore and pore assembly by a cholesterol-dependent cytolysin. J Biol Chem 2007;282:15709–15716. [PubMed: 17412689]

15. Song X, Xia B, Lasanajak Y, Smith DF, Cummings RD. Quantifiable fluorescent glycan microarrays. Glyco-conjugate J 2008;25:15–25.

16. Alberio L, Safa O, Clemetson KJ, Esmon CT, Dale GL. Surface expression and functional characterization of alpha-granule factor V in human platelets: effects of ionophore A23187, thrombin, collagen, and convulxin. Blood 2000;95:1694–1702. [PubMed: 10688826]

17. Remenyi G, Szasz R, Friese P, Dale GL. Role of mitochondrial permeability transition pore in coated-platelet formation. Arteriosci, Thromb Vasc Biol 2005;25:467–471. [PubMed: 15591217]

18. Shepard LA, Shatursky O, Johnson AE, Tweten RK. The mechanism of assembly and insertion of the membrane complex of the cholesterol-dependent cytolysin perfringolysin O: Formation of a large prepore complex. Biochemistry 2000;39:10284–10293. [PubMed: 10956018]

19. Boraston AB, Wang D, Burke RD. Blood group antigen recognition by a *Streptococcus pneumoniae* virulence factor. J Biol Chem 2006;281:35263–35271. [PubMed: 16987809]

20. Czajkowsky DM, Hotze EM, Shao Z, Tweten RK. Vertical collapse of a cytolysin prepore moves its trans-membrane *β*-hairpins to the membrane. EMBO J 2004;23:3206–3215. [PubMed: 15297878]

21. Harris RW, Sims PJ, Tweten RK. Kinetic aspects of the aggregation of *Clostridium perfringens* theta toxin on erythrocyte membranes: A fluorescence energy transfer study. J Biol Chem 1991;266:6936–6941. [PubMed: 2016307]

22. Hotze EM, Wilson-Kubalek EM, Rossjohn J, Parker MW, Johnson AE, Tweten RK. Arresting pore formation of a cholesterol-dependent cytolysin by disulfide trapping synchronizes the insertion of the transmembrane beta-sheet from a prepore intermediate. J Biol Chem 2001;276:8261–8268. [PubMed: 11102453]

23. Giddings KS, Zhao J, Sims PJ, Tweten RK. Human CD59 is a receptor for the cholesterol-dependent cytolysin intermedilysin. Nat Struct Mol Biol 2004;12:1173–1178. [PubMed: 15543155]

24. Heuck AP, Tweten RK, Johnson AE. Assembly and topography of the prepore complex in cholesterol-dependent cytolysins. J Biol Chem 2003;278:31218–31225. [PubMed: 12777381]

25. Ramachandran R, Heuck AP, Tweten RK, Johnson AE. Structural insights into the membrane-anchoring mechanism of a cholesterol-dependent cytolysin. Nat Struct Biol 2002;9:823–827. [PubMed: 12368903]

26. Ramachandran R, Tweten RK, Johnson AE. The domains of a cholesterol-dependent cytolysin undergo a major FRET-detected rearrangement during pore formation. Proc Natl Acad Sci USA 2005;102:7139–7144. [PubMed: 15878993]

27. Tweten RK. The cholesterol-dependent cytolysins; a family of versatile pore-forming toxins. Infect Immun 2005;73:6199–6209. [PubMed: 16177291]

28. Kawamura Y, Hou XG, Sultana F, Miura H, Ezaki T. Determination of 16S rRNA sequences of *Streptococcus mitis* and *Streptococcus gordonii* and phylogenetic relationships among members of the genus *Streptococcus*. Int J Syst Bacteriol 1995;45:406–408. [PubMed: 7537076]

29. Melo F, Feytmans E. Assessing protein structures with a non-local atomic interaction energy. J Mol Biol 1998;277:1141–1152. [PubMed: 9571028]

30. Merritt EA, Sixma TK, Kalk KH, van Zanten BA, Hol WG. Galactose-binding site in *Escherichia coli* heat-labile enterotoxin (LT) and cholera toxin (CT). Mol Microbiol 1994;13:745–753. [PubMed: 7997185]

31. Stein PE, Boodhoo A, Armstrong GD, Cockle SA, Klein MH, Read RJ. The crystal structure of pertussis toxin. Structure 1994;2:45–57. [PubMed: 8075982]

32. Olson R, Gouaux E. Crystal structure of the *Vibrio cholerae* cytolysin (VCC) pro-toxin and its assembly into a heptameric transmembrane pore. J Mol Biol 2005;350:997–1016. [PubMed: 15978620]

33. Clark GF, Krivan HC, Wilkins TD, Smith DF. Toxin A from *Clostridium difficile* binds to rabbit erythrocyte glycolipids with terminal Gal alpha 1–3Gal beta 1–4GlcNAc sequences. Arch Biochem Biophys 1987;257:217–229. [PubMed: 3115180]

34. Nesic D, Hsu Y, Stebbins CE. Assembly and function of a bacterial genotoxin. Nature 2004;429:429–433. [PubMed: 15164065]

35. Tateno H, Goldstein IJ. Molecular cloning, expression, and characterization of novel hemolytic lectins from the mushroom *Laetiporus sulphureus*, which show homology to bacterial toxins. J Biol Chem 2003;278:40455–40463. [PubMed: 12900403]

36. Rossjohn J, Buckley JT, Hazes B, Murzin AG, Read RJ, Parker MW. Aerolysin and pertussis toxin share a common receptor-binding domain. EMBO J 1997;16:3426–3434. [PubMed: 9218785]

37. Hakomori SI, Siddiqui B. Isolation and characterization of glycosphingolipid from animal cells and their membranes. Methods Enzymol 1974;32:345–367. [PubMed: 4374628]

38. Marcus DM. The ABO and Lewis blood-group system. Immunochemistry, genetics and relation to human disease. N Engl J Med 1969;280:994–1006. [PubMed: 4888078]

39. Inoue M, Nakayama M, Tanizawa O. Altered expression of Lewis blood group and related antigens in fetal, normal adult and malignant tissues of the uterine endometrium. Virchows Arch 1990;416:221–228.

40. Heller DS, Thung SN. Expression of Lewis(x) and Lewis(y) blood group related antigens in fetal livers. Pediat Pathol 1990;10:681–687.

41. Jass JR, Roberton AM. Colorectal mucin histochemistry in health and disease: a critical review. Pathol Int 1994;44:487–504. [PubMed: 7921193]

42. Abe K, Hakomori S, Ohshiba S. Differential expression of difucosyl type 2 chain (LeY) defined by monoclonal antibody AH6 in different locations of colonic epithelia, various histological types of colonic polyps, and adenocarcinomas. Cancer Res 1986;46:2639–2644. [PubMed: 3516384]

43. Sakamoto S, Watanabe T, Tokumaru T, Takagi H, Nakazato H, Lloyd KO. Expression of Lewisa, Lewisb, Lewisx, Lewisy, siayl-Lewisa, and sialyl-Lewisx blood group antigens in human gastric carcinoma and in normal gastric tissue. Cancer Res 1989;49:745–752. [PubMed: 2910493]

44. Appelmelk BJ, Simoons-Smit I, Negrini R, Moran AP, Aspinall GO, Forte JG, DeVries T, Quan H, Verboom T, Maaskant JJ, Ghiara P, Kuipers EJ, Bloemena E, Tadema TM, Townsend RR, Tyagarajan K, Crothers JM Jr, Monteiro MA, Savio A, DeGraaff J. Potential role of molecular mimicry between *Helicobacter pylori* lipopolysac-charide and host Lewis blood group antigens in autoimmunity. Infect Immun 1996;64:2031–2040. [PubMed: 8675304]

45. Dettke M, Palfi G, Loibner H. Activation-dependent expression of the blood group-related lewis Y antigen on peripheral blood granulocytes. J Leukocyte Biol 2000;68:511–514. [PubMed: 11037972]

46. Dettke M, Palfi G, Pursch E, Fischer MB, Loibner H. Increased expression of the blood group-related Lewis Y antigen on synovial fluid granulocytes of patients with arthritic joint diseases. Rheumatology (Oxford, England) 2001;40:1033–1037.

47. Polekhina G, Giddings KS, Tweten RK, Parker MW. Insights into the action of the superfamily of cholesterol-dependent cytolysins from studies of intermedilysin. Proc Natl Acad Sci USA 2005;102:600–605. [PubMed: 15637162]

48. Humphrey W, Dalke A, Schulten K. VMD: visual molecular dynamics. J Mol Graphics 1996;14:33–38. 27–38.

a

```
LLY MNQEKRLHRFVKKCGLGVCSAVVAAFLLNAQGVALATEQGNRPVETENIARGKQASQSST 60
ILY MKTKQNIARKLSRVVLLSTLVLSSAAPISAAFA-------------------------- 33
PLY M----------------------------------------------------------- 1
    *
                  A
LLY AYGGAATRAVDGNVDSDYGHHSVTHTNFEDNAWWQVDLGKTENVGKVKLYNRGDGNVANR 120
ILY ----------------------------------------------------------- 33
PLY ----------------------------------------------------------- 1

LLY LSNFDVVLLNEAKQEVARQHFDSLNGKAELEVFFTAKDARYVKVELKTKNTPLSLAEVEV 180
ILY -------------------------------------------------ETPTKPKA 41
PLY ----------------------------------------------------------- 1
                        A
LLY FRSATTQVGQDRTAPVVDQTSALKDYLFGLTYNPLDILTRKGETLENRYNTSAKEQNGEF 240
ILY AQTEKKPEKKPENSNSEAAKKALNDYIWGLQYDKLNILTHQGEKLKNHSSREAFHRPGEY 101
PLY ------------------ANKAVNDFILAMNYDKKKLLTHQGESIENRFIKEGNQLPDEF 43
                            *::*:: : *:  :**:*:** ::*:           *:
LLY VVVEKIKKTLSTGTADVSING--NQNVFLGGLYKANQNLLENQPELISLARAKGTVSVDL 298
ILY VVIEKKKQSISNATSKLSVSSANDDRIFPGALLKADQSLLENLPTLIPVNRGKTTISVNL 161
PLY VVIERRKRSLSTNTSDISVTATNDSRLYPGALLVDETLLENNPTLLAVDRAPMTYSIDL 103
    **:*: *:::*: *:  :*:    : :: * *  :: **** * *: *   * *:*
                Q DSR    D     S     R
LLY PGMIHSENKIEA-NPTTSGMQEAMNTLVEKWTKNYSSSHSVPARVQYESTTAYSMNQLKA 357
ILY PGLKNGESNLTVENPSNSTVRTAVNNLVEKWIQKYSKTHAVPARMQYESISAQSMSQLQA 221
PLY PGLASSDSFLQVEDPSNSSVRGAVNDLLAKWHQDYGQVNNVPARMQYEKITAHSMEQLKV 163
    **:   :  :   :*: *  :: *:* *: ** : *   : ****:*** :* ** **:
LLY KFGADFEKAGAPLKIDFEAVQKGEKQIEVVNFKQIYYTATFDAPTNPAAVFDKSVTPEDL 417
ILY KFGADFSKVGAPLNVDFSSVHKGEKQVFIANFRQVYYTASVDSPNSPSALFGSGITPTDL 281
PLY KFGSDFEKTGNSLDIDFNSVHSGEKQIQIVNFKQIYYTVSVDAVKNPGDVFQDTVTVEDL 223
    ***:** * *  * :** :*: **** : **:*:*** : *:   *  :* :* **
                        A
LLY KQRGVDSQTPPVYVSNVSYGRQIYVKFESTSKSTELKAAINAVIKGATIAPNSEWSRLLK 477
ILY INRGVNSKTPPVYVSNVSYGRAMYVKFETTSKSTKVQAAIDAVVKGAKLKAGTEYENILK 341
PLY KQRGISAERPLVYISSVAYGRQVYLKLETTSKSDEVEAAFEALIKGVKVAPQTEWKQILD 283
    :**: :: * **:* *:**** :*:*:*:**** ::**::::** : :*: :*
LLY NTSVTAVIVGGNASGAAKVVTGTVENLKELIREGANFSAQSPAVPISYKTAFLKDNAQAT 537
ILY NTKITAVVLGGNPGEASKVITGNIDTLKDLIQKGSNFSAQSPAVPISYTTSFVKDNSIAT 401
PLY NTEVKAVILGGDPSSGARVVTGKVDMVEDLIQEGSRFTADHPGLPISYTTSFLRDNVVAT 343
    ** : **::**:    ::*:** :: ::**:*: *:*: * :**** *:*::** **
                                       V
LLY LQNSTDYIETKVTSYKNGFLKLHHKGAYIARYYIYWDEITYDEQGNPEIRSRQWEDNGKN 597
ILY IQNNTDYIETKVTSYKDGALTLNHDGAFVARFYVVWEELGHDADGYETIRSRSWSGNGYN 461
PLY FQNSTDYVETKVTAYRNGDLLLDHSGAYVAQYYITWDELSYDHQGKEVLTPKAWDRNGQD 403
    :** ***:****:*::* * * **::*::* * *:*: :* :*   : * * **  *:
LLY RTSGFQTEIQFRGNVRNLRIKVG|EKTGLVWEPWR|TVYNRTDLPLVQQRTITHWGTTLNPK 657
ILY RGAHYSTTLRFKGNVRNIRVKVG|GATGLAWEPWR|LIYSKNDLPLVPQRNISTWGTTLHPQ 521
PLY LTAHFTTSIPLKGNVRNLSVKIR|ECTGLAWEWWR|TVYEKTDLPLVRKRTISIWGTTLYPQ 463
    :  : *  : ::*****: :*: *** *** ** :* : ***** :* *: ***** *:

LLY VDEKIVNE--- 665
ILY FEDKVVKDNTD 532
PLY VEDKVEND--- 471
    ::*: ::
```

b

```
LLYLec  T-EQGNRPVETENIA-RGKQASQSSTAYGGAAAR-----AVDGNVDSDYGHHSVTHTNFE 89
AAA    VIPEG---YTQENVAVRGK-ATQSAQLRGEHAANSEASNAIDGNRDSNFYHGSCTHSSGQ 56
       :*      **:* *** *:**:   *  **       *:*** **:: * * **:  :

LLYLec  DNAWWQVDLGKTENVGKVKLYNRGDGNVANRLSNFDVVLLNEAKQEVARQHFDSLNGK-- 147
AAA    ANPWWRVDLLQVYTITSVTITNRGDC-CGERISGAEINIGQHLASNGVNNPECSVIGSMA 115
       * **:***  : * *:****  :*:*  :: :  :    :  *:   *

LLYLec  -AELEVFF--TAKAARYVKVELKTKNTPLSLAEVEVFRSATTVGQDRTAPVVD 198
AAA    TGETKTFHCPAPMIGRYVVTYLPTSES-LHLCEVEV--------NVDK--PAAA 158
       *  :  *   :   *** * * :: * * ****        *:  *
```

c

```
LLYLec   TEQGNRPVETENIARGKQASQSSTAYGGAAAARAVDGNVDSDYGHHSVTHTNFEDNAWWQV 96
SP2159  EEDIDKITEDKVVSTNKVATQSSTNYEGVAALAVDGNKDGDYGHHSVTHTKADSNAWWQV 810
        *:  ::   * : :: *  *:**** * * **  ***** * *********T: : ******

LLYLec   DLGKTENVGKVKLYNRGDGNVANRLSNFDVVLLNEAKQEVARQHFDSL-NGKAELEVFFT 155
SP2159  DLGEEFTVSKVDIYNRTDAE-PQRLSNFDVIFLSSSGEEVFRRHFDKVADGLLSLKV--P 867
        ***:    *  **:*** *  : :*******:*  : :** *:*** : :*    *:*

LLYLec   AKAARYVKVELKTKNTPLSLAEVEVFRSATTQVGQDRTAPVVD 198
SP2159  SVGAKLVKIELKSAAIPLSLAEVEVYGSKRTPKKLSNIALTKE 910
        : *: **;***: ********: * *        *   :
```

Figure 1.
Primary structure of LLY. (a) The primary structure of LLY and its comparison with the primary structures of ILY and PLY. Comparison of the primary structure of LLY[Lec] with that of the (b) *A. anguilla* agglutinin (AAA) (10) and (c) the glycan binding domain of the family 98 glycoside hydrolases from *S. pneumoniae* (SP2159) (19). The letters above the LLY sequence in panel a represent the amino acid differences with the GenBank sequence of Sm-hPAF (accession number AB051299.1). Homology comparisons were carried out using CLC Free Workbench version 4.6 (CLCBio). The conserved undecapeptide sequence of the CDCs is boxed in panel a. The conserved active site residues of AAA are bolded and underlined in panels b and c. Conserved residues (*), conservative substitutions (:).
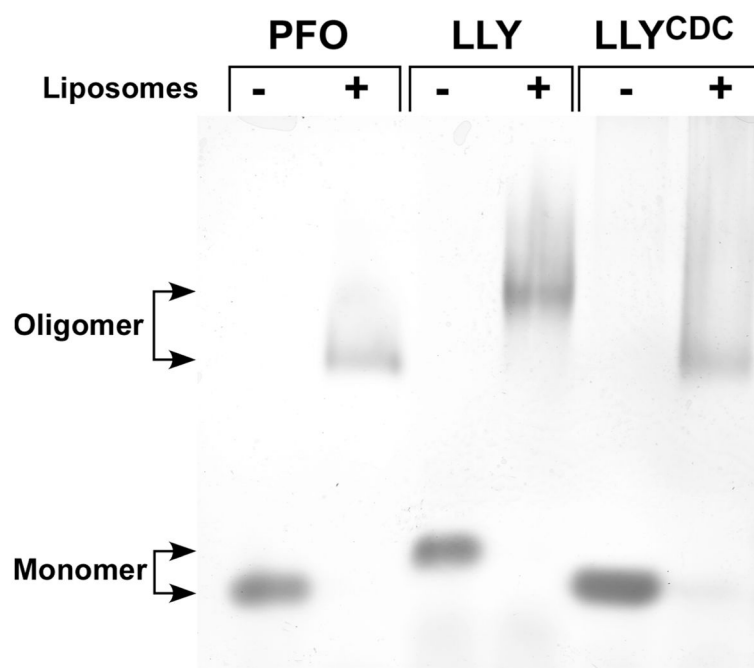
Figure 2.
Oligomer formation by LLY. Purified PFO, LLY, and LLY^{CDC} were incubated in the absence and presence cholesterol-rich liposomes, and the monomer and oligomer species were separated by SDS–AGE. Shown is the Coomassie stained gel. The smearing of the oligomer bands results from the presence of the liposome-derived lipids in the oligomer samples.
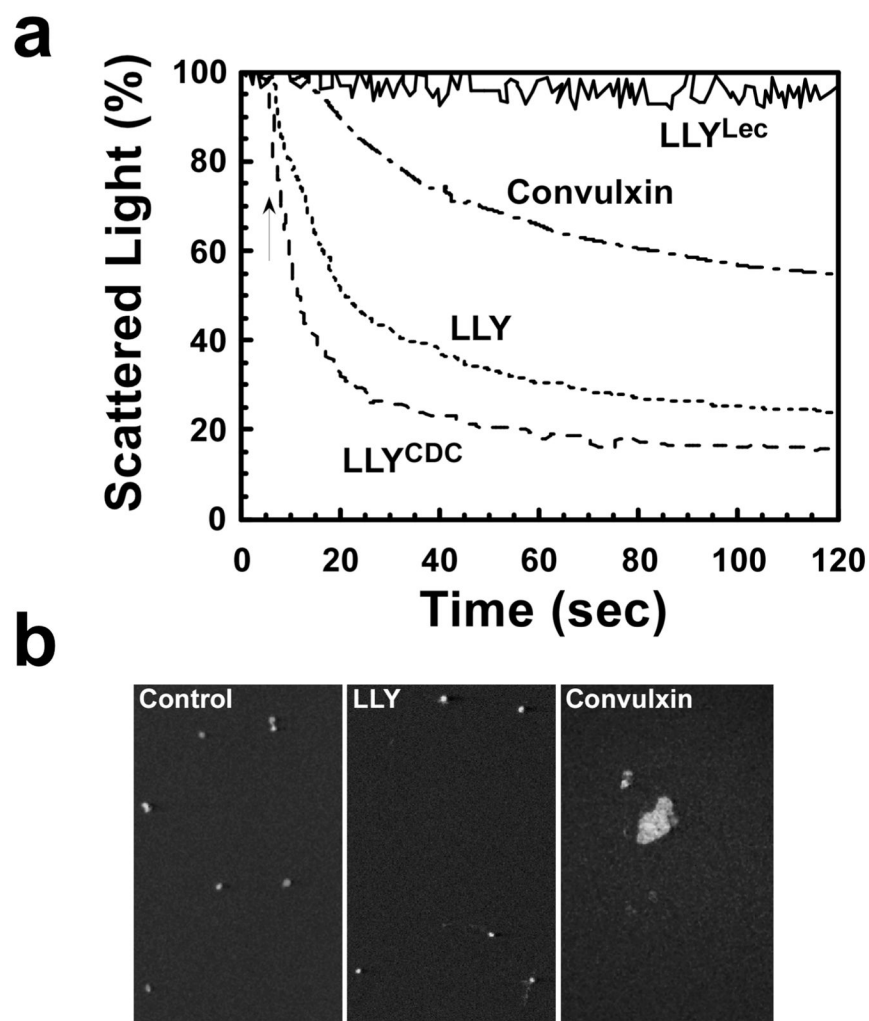
Figure 3.
Platelet aggregation by LLY. Shown in (a) are the aggregometer recordings for platelets treated with LLY (71 nM), LLY^{CDC} (95 nM), and LLY^{Lec} (280 nM) and the positive control convulxin (500 ng/mL). Shown in (b) are confocal microscopic images of untreated, LLY-treated, and convulxin-treated platelets. These fields are representative of 12 separate fields.
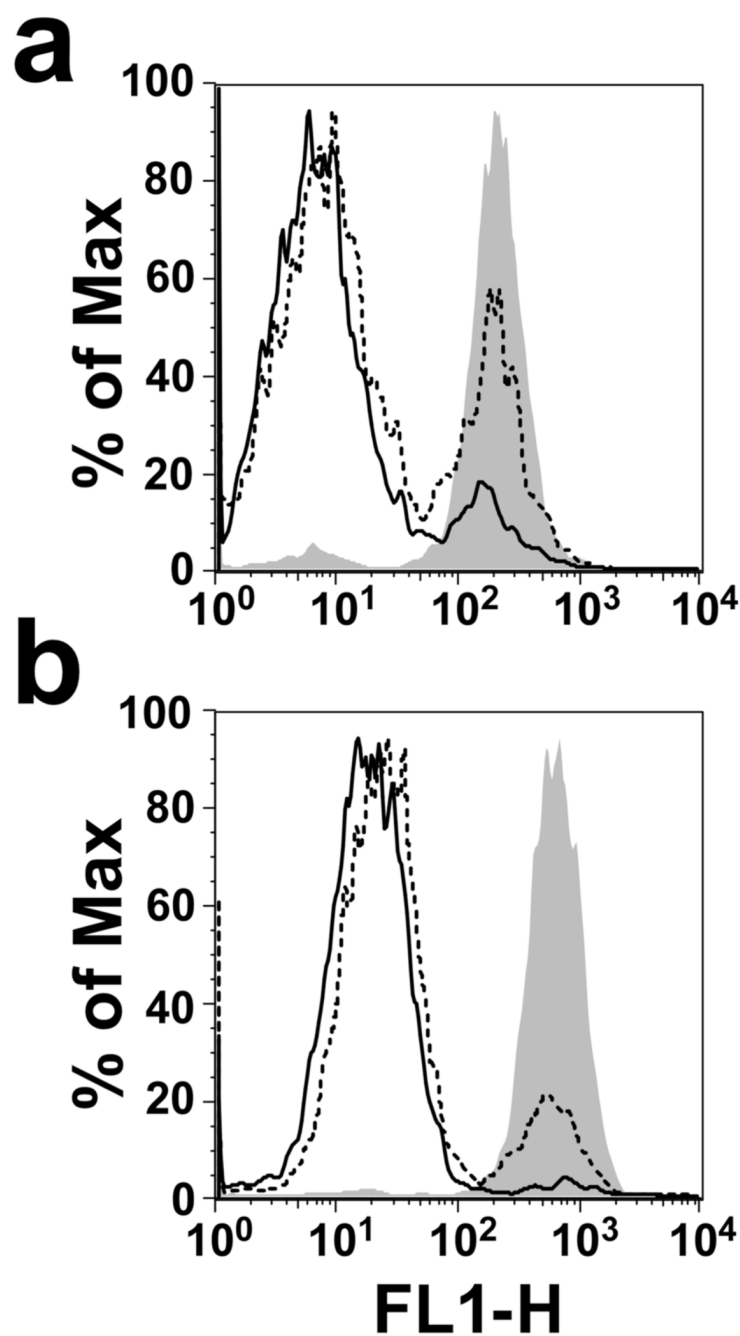
Figure 4.
Calcein release from LLY-treated platelets. Calcein-loaded platelets were assayed by flow cytometry before (shaded peak) and after treatment with 0.7 nM (dashed line) or 1.4 nM (solid line) LLY (a) or LLY^{CDC} (b).
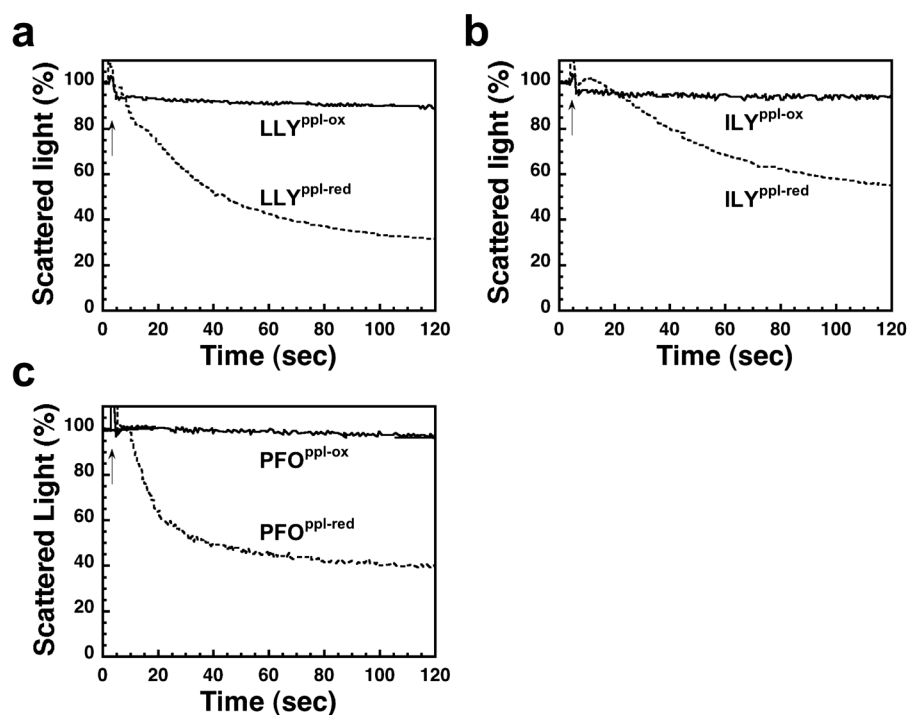
Figure 5.
Platelet lysis requires pore formation. Shown are aggregometer readings for platelets treated with prepore locked mutants of LLY (a), ILY (b), and PFO (c) in their oxidized (LLY^{ppl-ox}, ILY^{ppl-ox}, and PFO^{ppl-ox}) and reduced forms (LLY$^{ppl-red}$, ILY$^{ppl-red}$, and PFO$^{ppl-red}$). Conditions were similar to those in Figure 3a; all toxins were added at approximately 70 nM. The reduction of the disulfide allows each prepore-locked mutant to convert to the pore complex.
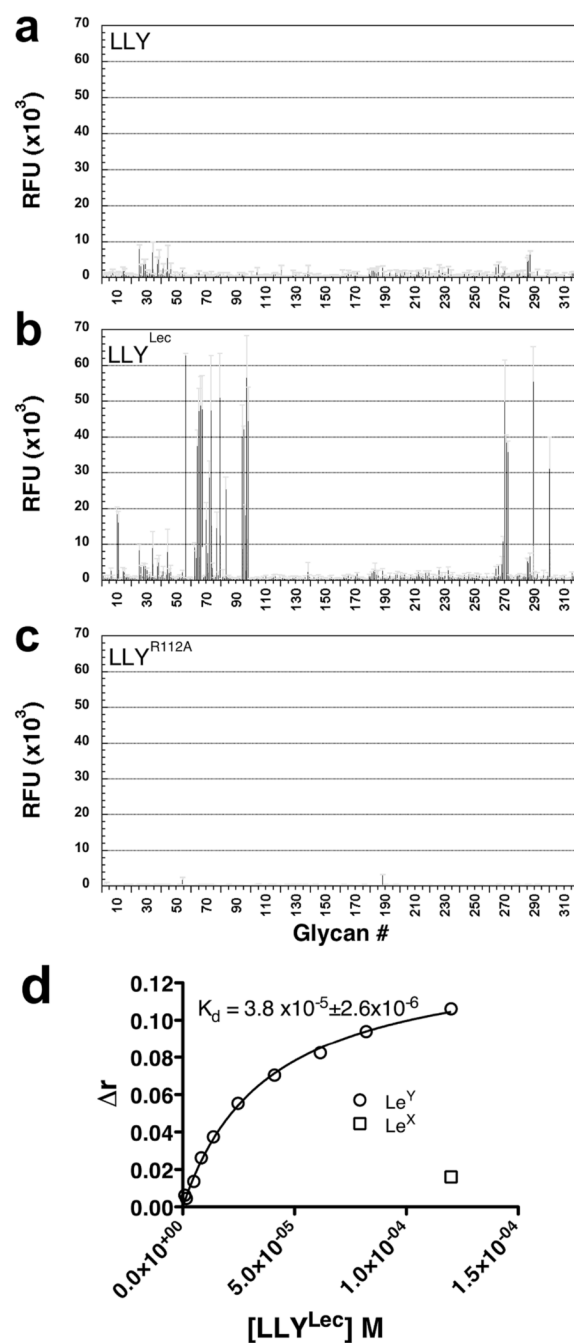
Figure 6.
Glycan binding by LLY, LLY^{Lec}, and LLY$^{Lec-R112A}$. Version 3.0 of the printed glycan microarray, containing 320 eukaryotic-derived glycans (see Methods for a link to the full list of glycans on this array), was probed with fluorescently tagged (Alexa-488) versions of (a) LLY (670 nM), (b) LLY^{Lec} (560 nM), and (c) LLY$^{Lec-R112A}$ (560 nM) that had been labeled at the cysteine-substituted Gln-190. Standard error of the mean is shown as gray error bars. Note: The microarray analyses herein were carried out using the updated version 3.0 of the glycan array whereas the results in Table 2 were obtained using version 2.1. This was a result of a change in the microarray version during the course of these studies. There are only five differences in fucose-containing glycans in the two versions. Only two of these glycans,

numbers 290 and 301 on the version 3.0 array, contain the H-antigen structure and were shown to be bound by LLY^{Lec} whereas the other three glycans were not (data not shown). In panel d the K_d of the Le^y–LLY^{Lec} interaction was determined by measuring changes in the anisotropy (Δr) of Le^y (kept constant at 167 nm) in the presence of LLY^{Lec} that was varied from 300 nM to 120 μM. Le^x incubated with the highest concentration of LLY (120 μM) exhibited a Δr of $\approx$10% of that observed for Le^y.
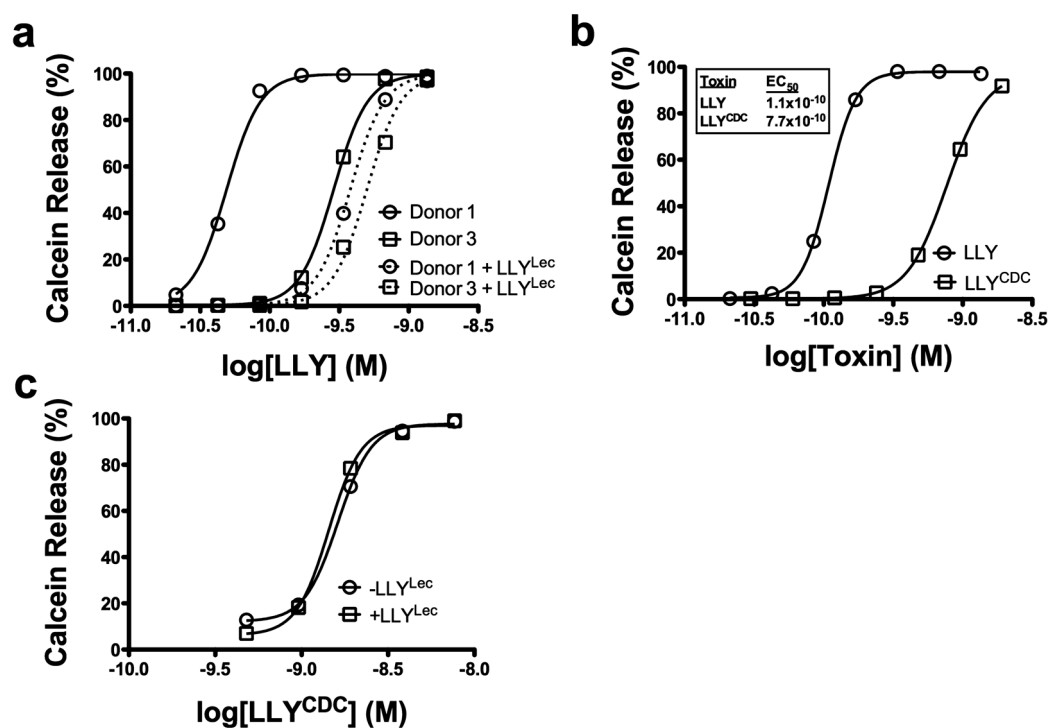
Figure 7.
The glycan-binding domain of LLY modulates pore-forming activity. LLY-dependent calcein release from calcein-loaded PRP was measured by flow cytometry. (a) LLY-dependent calcein release from platelets of high (donor 1) and low responding donors (donor 3) which were preincubated without (solid lines) or with (dashed lines) LLY[Lec] (56 nM). No change is observed with LLY[Lec] alone (not shown). (b) Calcein release from platelets treated with LLY or LLY[CDC]. (c) Same as the experiments shown in (a) with donor 1 platelets except that LLY[CDC] was substituted for LLY.
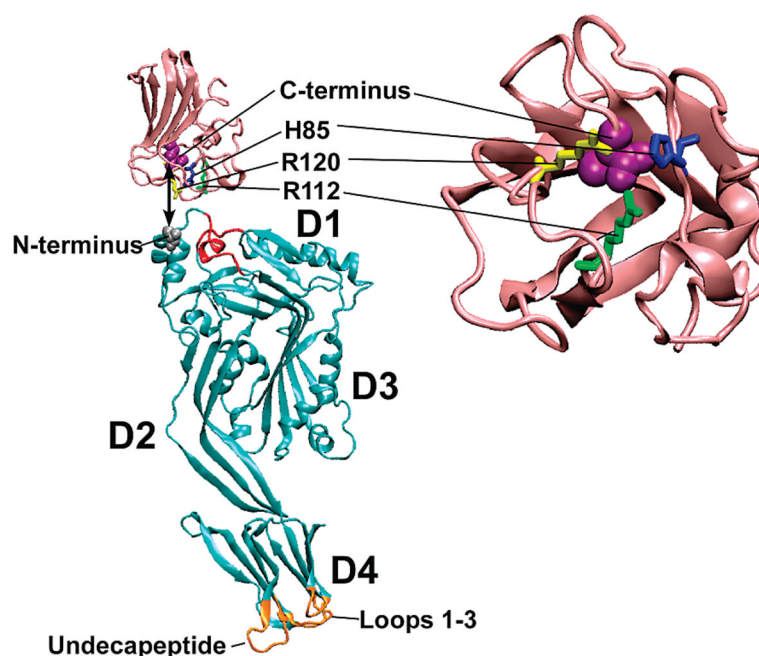
Figure 8.
Molecular models of LLY^CDC and LLY^Lec. Shown are the ribbon representations of the LLY^CDC (cyan) and LLY^Lec (pink) molecular models generated by Swiss Model (swissmodel.expasy-.org). The LLY^CDC model was generated using the ILY crystal structure (47) as the template whereas the LLY^lec was modeled based on the structure of the Le^y-binding module of a *S. pneumoniae* virulence factor of the family 98 glycoside hydrolases (19). The locations are shown for the fucose-binding residues [His-85 (blue), Arg-112 (yellow), and Arg-120 (green)] and the C-terminal residue (space filled, magenta) of LLY^Lec and the amino-terminal residue of LLY^CDC (space filled, gray). The L1-L3 loops and undecapeptide at the tip of domain 4 are shown in gold. The red-colored regions of the LLY^CDC structural model exhibited a nonfavorable energy environment when analyzed with ANOLEA (29). Molecular structures were drawn with VMD (48).
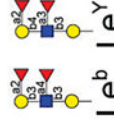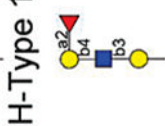
Table 1

Hemolytic Activity of LLY and Related CDCs Used in This Study[a]

CDC	HD$_{50}$ (pM)
ILY	1.1
PFO	0.8
LLY	4.1
LLY^{CDC}	4.4

[a]The relative HD$_{50}$ (hemolytic dose for 50% lysis of a standard erythrocyte suspension; see Methods) for each CDC used in these studies is provided.

Table 2

LLY^Lec Preferentially Binds Le^Y and Le^b Glycans[a]

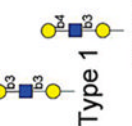| Glycan Family	Glycan Structure	Glycan #	560 nM AVG RFU	560 nM %CV	56 nM AVG RFU	56 nM %CV	5.6 nM AVG RFU	5.6 nM %CV
Le^b / Le^Y	Fucα1–2Galβ1–4(Fucα1–3)GlcNAcβ-Sp8	1	42035	1004	50113	18	16748	3
	Fucα1–2Galβ1–4(Fucα1–3)GlcNAcβ-Sp0	2	52303	8	40704	6	15357	11
	Fucα1–2Galβ1–3Fucα1–4)GlcNAcβ-Sp8	3	44801	7	44960	9	11763	5
	Fucα1–2Galβ1–4(Fucα1–3)GlcNAcβ1–3Galβ1–4(Fucα1–3)GlcNAcβ-Sp0	4	42253	4	54171	10	9445	10
	Fucα1–2Galβ1–4(Fucα1–3)GlcNAcβ1–3Galβ1–4(Fucα1–3)GlcNAcβ1–3Galβ1–4(Fucα1–3)GlcNAcβ-Sp0	5	49653	11	54594	11	9201	3
	Galα1–3(Fucα1–2)Galβ1–4(Fucα1–3)GlcNAcβ-Sp0	6	43236	3	39872	2	9022	5
	GalNAcα1–3(Fucα1–2)Galβ1–4(Fucα1–3)GlcNAcβ-Sp0	7	45556	4	37850	1	5506	2
Bld Grp B	Galα1–3(Fucα1–2)Galβ-Sp8	8	42263	30	28788	6	2936	5
	Galα1–3(Fucα1–2)Galβ1–4Glcβ-Sp0	9	55729	9	11208	14	846	26
	Galα1–3(Fucα1–2)Galβ1–3GlcNAcβ-Sp0	10	35310	5	9312	19	743	17
	Galα1–3(Fucα1–2)Galβ1–4GlcNAc-Sp0	11	9081	8	2701	9	338	26
Bld Grp A	GalNAcα1–3(Fucα1–2)Galβ-Sp8	12	13806	9	3635	14	282	18
	GalNAcα1–3(Fucα1–2)Galβ1–3GlcNAcβ-Sp0	13	203	18	247	34	304	59
	GalNAcα1–3(Fucα1–2)Galβ1–4Glcβ-Sp0	14	617	11	302	36	97	12
H-Type 1	Fucα1–2Galβ-Sp8	15	51057	11	17066	19	1443	13
	Fucα1–2[6OSO3]Galβ1–4[6OSO3]Glc-Sp0	16	35842	10	12584	14	486	47
	Fucα1–2-Galβ1–4[6OSO3]Glc-Sp0	17	23604	8	9152	9	176	65
	Fucα1–2Galβ1–4Glcβ-Sp0	18	17933	1	5716	12	537	14
	Fucα1–2Galβ1–4GlcNAcβ-Sp0	19	13896	12	3452	17	327	13
	Fucα1–2-(6OSO3)-Galβ1–4Glc-Sp0	20	13295	15	2345	90	56	42
H-Type 2	Fucα1–2Galβ1–3GlcNAcβ-Sp0	21	8226	10	1727	19	214	8
	Fucα1–2Galβ1–3GlcNAcβ-Sp8	22	7311	8	2133	14	164	73
	Fucα1–2Galβ1–4[6OSO3]GlcNAc-Sp8	23	5908	16	1845	25	276	22
	Fucα1–2Galβ1–4GlcNAcβ1–3Galβ1–4GlcNAc-Sp8	24	5045	10	1175	13	147	36
	Fucα1–2Galβ1–4GlcNAcβ1–3Galβ1–4GlcNAcβ-Sp0	25	135	27	478	40	208	40
	Fucα1–2Galβ1–3GlcNAcβ1–3Galβ1–4Glcβ-Sp8	26	215	42	163	33	135	33
Le^a Le^X	Fucα1–4GlcNAcβ-Sp8	27	189	134	211	80	78	37
	Galβ1–3(Fucα1–4)GlcNAcβ-Sp8	28	237	61	101	15	144	88
	Neu5Acα2–3Galβ1–3(Fucα1–4)GlcNAcβ-Sp8	29	116	41	212	26	112	37
	Fucα1–3GlcNAcβ-Sp8	30	169	52	164	38	232	26
	Galβ1–4(Fucα1–3)GlcNAcβ-Sp8	31	91	79	184	8	194	26
Type 1	Neu5Acα2–3Galβ1–4(Fucα1–3)GlcNAcβ1–3Galβ-Sp8	32	187	75	98	61	89	36
	Neu5Acα2–3Galβ1–4GlcNAcβ1–3Galβ1–3Galβ1–4GlcNAcβ-Sp0	33	281	49	169	27	111	39
	Galβ1–4GlcNAcβ1–3Galβ1–4GlcNAcβ1–3Galβ1–4GlcNAcβ-Sp0	34	217	37	189	50	152	60
	Galβ1–4GlcNAcβ1–3Galβ1–4GlcNAcβ-Sp0	35	183	26	120	35	170	48
	NeuAcα2–3Galβ1-SGlcNAcβ1–3Galβ1–4GlcNAcβ-Sp0	36	194	33	147	49	117	49
	Galβ1-SGlcNAcβ1–3Galβ1–4Glcβ-Sp10	37	340	77	170	60	172	34
Type 2	Galβ1–3GlcNAcβ1–3Galβ1–3GlcNAcβ-Sp0	38	333	123	123	37	79	79
Other	α-L-Fuc-Sp8	39	3038	14	1435	36	326	28
	[3OSO3]Galβ1–4(6OSO3)Glcβ-Sp8	40	2745	28	848	11	397	17
	Transferrin	41	4066	31	1679	34	905	20

NIH-PA Author Manuscript   NIH-PA Author Manuscript   NIH-PA Author Manuscript

Glycan Family	Glycan #	Glycan Structure	560 nM		56 nM		5.6 nM	
			AVG RFU	%CV	AVG RFU	%CV	AVG RFU	%CV
	42	Galβ1–4(Fucα1–3)GlcNAcβ1–4Galβ1–4(Fucα1–3)GlcNAcβ1–4Galβ1–4(Fucα1–3)GlcNAcβ-Sp0	522	68	138	16	216	48
	43	NeuAcα2–3Galβ1–3(Fucα1–4)GlcNAcβ1–3Galβ1–4(Fucα1–3)GlcNAcβSp0	407	28	171	25	122	51
	44	Galβ1–4(Fucα1–3)GlcNAcβ1–3Galβ1–3(Fucα1–4)GlcNAcβ-Sp0	649	97	490	46	169	42
	45	Galβ1–3(Fucα1–4)GlcNAcβ1–3Galβ1–3(Fucα1–4)GlcNAcβ-Sp0	254	111	215	46	155	67
Difucosylated, lacking Blood Group H	46	Galβ1–3(Fucα1–4)GlcNAcβ1–3Galβ1–4(Fucα1–3)GlcNAcβ-Sp0	223	40	167	49	197	27
	47	Galβ1–4(Fucα1–3)GlcNAcβ1–4GlcNAoβ1–4(Fucα1–3)GlcNAcβ-Sp0	234	31	418	24	229	37
	48	Neu5Acα2–6Galβ1–4GlcNAcβ1–3Galβ1–4(Fucα1–3)GlcNAcβ1–3Galβ1–4(Fucα1–3)GlcNAcβ-Sp0	422	104	158	18	93	32
	49	Galβ1–4GlcNAcβ1–3Galβ1–4(Fucα1–3)GlcNAcβ1–3Galβ1–4(Fucα1–3)GlcNAcβ-Sp0	105	34	166	31	137	29
	50	Neu5Acα2–3Galβ1–4(Fucα1–3)GlcNAcβ1–3Galβ1–4(Fucα1–3)GlcNAcβ1–4(Fucα1–3)GlcNAcβ-Sp0	23	517	287	58	170	15

[a] Version 2.1 of the printed glycan microarray (Consortium for Functional Glycomics) was probed with Alexa-488 labeled LLY^{Lec}-Q190C at 560, 56, and 5.6 nM. To demonstrate specificity of binding by LLY^{Lec}, all glycans that were bound at the highest LLY^{Lec} concentration are shown as well as related glycans that were not bound or weakly bound. The average RFU (from four or six analysis with high and low values eliminated) for each bound glycan was determined as described in Methods and the % CV (100 × standard deviation ÷ average) provides an indication of the precision of each measurement. All other glycans on the version 2.1 array probed at the highest concentration of ILY^{Lec} did not exhibit signals above background. AVG RFU is average relative fluorescence units; SP, spacer arm or linker between glycan and surface of the array; SP0, –CH2CH2NH2; and SP8, –CH2CH2CH2NH2. Key: yellow circles, galactose; GalNac; yellow squares, GalNac; red triangles, fucose; blue squares, GlcNAc.